INSTITUTE OF PHYSICS PUBLISHING JOURNAL OF PHYSICS A: MATHEMATICAL AND GENERAL

J. Phys. A: Math. Gen. **36** (2003) 10667–10681 PII: S0305-4470(03)61201-1

A consequence of local equilibration and heterogeneity in glassy materials

Ludovic Berthier

Theoretical Physics, 1 Keble Road, Oxford, OX1 3NP, UK
and
Laboratoire des Verres, Université Montpellier II, 34095 Montpellier, France

Received 21 March 2003
Published 15 October 2003
Online at stacks.iop.org/JPhysA/36/10667

Abstract

The existence of a generalized fluctuation–dissipation theorem observed in simulations and experiments performed in various glassy materials is related to the concepts of local equilibration and heterogeneity in space. Assuming the existence of a dynamic coherence length scale up to which the system is locally equilibrated, we extend previous generalizations of the FDT relating static to dynamic quantities to the physically relevant domain where asymptotic limits of large times and sizes are not reached. The formulation relies on a simple scaling argument and thus does not have the character of a theorem. Extensive numerical simulations support this proposition. Our results quite generally apply to systems with slow dynamics, independently of the space dimensionality, the chosen dynamics or the presence of disorder.

PACS numbers: 05.70.Ln, 75.10.Nr, 75.40.Mg

How slow the wind
How slow the sea
E Dickinson

Materials can be far from their equilibrium state for two main reasons. First, the relaxation time can be very large compared to the experimental time scale and the system does not reach equilibrium. This is typically the case for a liquid supercooled through its melting transition below its glass transition. The glass state is thus a non-stationary non-equilibrium state, where the glass is said to age. 'Glass phases' are extremely commonly encountered in condensed matter [1]. Secondly, when some external drive mechanism is applied to the system, it also leaves its equilibrium state. Typical situations can be driven interfaces, or soft materials perturbed by a mechanical flow. In this paper, we consider these two types of situations in the specific case of systems with slow dynamics. We discuss theoretically and numerically the existence and formulation of a generalization of the equilibrium fluctuation–dissipation theorem and its link to equilibrium properties.

Important results for the understanding of the non-equilibrium dynamics of glassy materials have been obtained in the last decade from the asymptotic solution of the dynamics of various infinite-range glassy models in the two types of situations described above [2]. It is established that much information on the dynamics is gained by studying two-time correlation and response functions, the relationship between them and the link between dynamic and static properties. In the case of an ageing dynamics, for instance, two-time functions explicitly retain a dependence on their two-time arguments, and conjugated correlation and response functions do not satisfy the relation they follow at equilibrium, the fluctuation–dissipation theorem (FDT). In the case of a driven dynamics, time translation invariance might be preserved even in the glassy phase, but the equilibrium FDT is not satisfied.

These 'mean-field' results have been used as a guide to interpret numerical and experimental studies of realistic glassy materials [3]. However, since no exact solution is known in that case, a naive mean-field interpretation of experimental results can be misleading. It is our aim to discuss the interpretation of experimental and numerical measurements of correlation and response functions in terms of static quantities. For this purpose, we extend the previous analysis to the physically relevant domain where large times and sizes are not accessible. Our approach, which relies on the concepts of a spatially local equilibration and heterogeneity of the system, closely follows the line of thought suggested in [4–10], where the need to take into account spatial aspects of slow dynamics was already emphasized in this particular context.

The paper is organized as follows. In section 1, we define the static and dynamic quantities of interest and briefly review the known relevant results. In section 2, we use a scaling argument to support our generalization of the FDT. Numerical simulations of ageing and driven dynamics in a spin glass model in finite spatial dimensions $d = 3$ and $d = 4$ are reported in section 3. Section 4 concludes the paper.

1. Generalized FDT: what do we know?

In this section, we introduce the basic concepts and quantities of interest for this paper. The exact results obtained in infinite-range glass models are first presented. We then review the argument given to support a possible larger validity of the mean-field results, and conclude the section with the experimental and numerical evidence available. The goal of this section is also to recall what is known, what is only supposed and most importantly to emphasize what is not known.

1.1. Infinite-range glass models

The solution of the non-equilibrium dynamics of infinite-range glass models consists of the asymptotic analysis of coupled dynamical equations involving two-time correlation functions, $C(t_1, t_2)$, and their thermodynamically conjugated response functions, $R(t_1, t_2)$ [11]. Alternatively, integrated responses, or susceptibilities, $\chi(t_1, t_2) = \int_{t_2}^{t_1} \mathrm{d}t' R(t_1, t')$, can be studied, with the advantage that $\chi(t_1, t_2)$ is easier to measure in a simulation or an experiment. Adopting notation appropriate to magnetic systems, those functions read for instance

$$C(t_1, t_2) = \frac{1}{N} \sum_{i=1}^{N} s_i(t_1) s_i(t_2) \tag{1}$$

$$R(t_1, t_2) = \frac{1}{N} \sum_{i=1}^{N} \left. \frac{\partial s_i(t_1)}{\partial h_i(t_2)} \right|_{h=0} \tag{2}$$

for a system composed of N spins s_i ($i = 1, \ldots, N$). The fields h_i are thermodynamically conjugated to the spins. Since (1) and (2) are self-averaging, no average of any kind is required if the thermodynamic limit, $N \to \infty$, is taken.

It turns out that in infinite-range glass models, a generalized form of the FDT is satisfied in the asymptotic limit of large times in the ageing case, or small driving forces for the driven case. The limits respectively read $t_1, t_2 \to \infty$ with $C(t_1, t_2)$ fixed, or $\varepsilon \to 0$ with $C(t_1 - t_2)$ fixed, where ε generically refers to the amplitude of the driving force (see below for examples). This asymptotic form of the FDT reads

$$R(t_1, t_2) = \frac{X[C(t_1, t_2)]}{T} \frac{\partial C(t_1, t_2)}{\partial t_2} \tag{3}$$

where T is the temperature, and $X(C)$ is called the fluctuation–dissipation ratio (FDR). The equilibrium FDT is recovered when $X(C) = 1$. The finding of a generalized FDT for non-equilibrated systems suggests the possibility of developing a non-equilibrium extension of standard statistical mechanics or thermodynamics. In particular, the quantity T/X has been shown to play the role of a non-equilibrium effective temperature for the slow modes of the system [12], leading to an important body of related works [13].

Moreover, in infinite-range glass models which statically exhibit a full replica symmetry breaking pattern, the new dynamical quantity $X(C)$ was found to be directly related to the static order parameter involved in the replica symmetry breaking, the distribution of overlaps $P(q)$, through the very simple relation [11],

$$X(C) = \int_0^C \mathrm{d}q' P(q'). \tag{4}$$

The 'Parisi function' is defined as

$$P(q) = \lim_{N\to\infty} \left\langle \delta \left(\frac{1}{N} \sum_{i=1}^{N} s_i^\alpha s_i^\beta - q \right) \right\rangle \tag{5}$$

where s_i^α denotes the value of spin i in the configuration α, and $\langle \cdots \rangle$ represents an average over configurations (α, β) weighted by their Boltzmann probability.

Equation (4) has a remarkable form, since it relates two quantities of completely different origin. The FDR on the left-hand side of (4) is measured in the off-equilibrium dynamics, while the Parisi function on the right-hand side is computed statically using the equilibrium Gibbs measure. Note also that the computation of $X(C)$ does not involve replicas.

Finally, we recall the remarkable result that a generalized FDT as in equation (3) is asymptotically obeyed in the case of the driven dynamics [12, 14], with the same value of the FDR, so that equation (4) remains unchanged in that case [15].

1.2. Stochastic stability

Further developments have taken a more speculative form, in the sense that no exact result has been obtained for finite-dimensional models. However, it was argued that equation (4) is generally true for finite-dimensional glassy systems [3]. We now briefly review the formal derivation of this result to emphasize the main hypotheses which are made. Following [11], the generalized susceptibilities χ^r are first introduced:

$$\chi^r = \frac{r!}{N^{r-1}} \sum_{i_1 < \cdots < i_r} \left. \frac{\partial s_{i_1} \cdots s_{i_r}}{\partial h_{i_1 \cdots i_r}} \right|_{h=0}. \tag{6}$$

The 'derivation' of equation (4) simply consists of the comparison between a static and a dynamic computation of χ^r [3]. A static average gives

$$\langle \chi^r \rangle_{\rm stat} = \lim_{N\to\infty} \lim_{t\to\infty} \langle \chi^r(t) \rangle = \frac{1}{T} \int_0^1 {\rm d}q\, P(q)(q^r - 1). \tag{7}$$

A dynamical average leads instead to

$$\langle \chi^r \rangle_{\rm dyn} = \lim_{t\to\infty} \lim_{N\to\infty} \langle \chi^r(t) \rangle = \frac{1}{T} \int_0^1 {\rm d}C \frac{{\rm d}X(C)}{{\rm d}C} (C^r - 1). \tag{8}$$

Equation (4) directly follows by requiring the equality $\langle \chi^r \rangle_{\rm stat} = \langle \chi^r \rangle_{\rm dyn}$ for all r.

There are, however, several assumptions in this derivation. First, one assumes that a non-trivial form of the FDT given by equation (3) is valid in the large-time limit. Similarly, the static computation is performed in the thermodynamic limit, $N \to \infty$. A third assumption is that static and dynamic calculations give the same result. This can be justified by a standard nucleation argument [3], although exceptions are known [11]. The last and strongest hypothesis has been called 'stochastic stability' [3]. The name originates from the fact that the susceptibility (6) probes the behaviour of the system under the random perturbation

$$H_{\rm perturbation} = \delta \sum_{i_1 < \cdots < i_r} h_{i_1 \cdots i_r} s_{i_1} \cdots s_{i_r} \tag{9}$$

in the limit $\delta \to 0$. Here, the field $h_{i_1 \cdots i_r}$ is a random Gaussian variable of mean 0 and variance $r!/(2N^{r-1})$. Stochastic stability implies thus that the limits $\delta \to 0$ (or equivalently $h \to 0$ in equation (6)), $N \to \infty$, and $t \to \infty$ can all be inverted. This last assumption is completely uncontrolled, so that equation (4) is made physically plausible by this calculation, but has no 'theorem' character. A measurable test of this last hypothesis in a realistic system is to check relation (4) it implies, thus making the argument a bit circular. Interesting examples and counterexamples were discussed in detail in [3].

1.3. Numerical and experimental results

Since the generalization of the FDT through equations (3) and (4) cannot be rigorously proved, numerical simulations and experiments are necessary in order to make some progress. The advantage of simulations is that both equations can be separately checked, while experiments can obviously not compare dynamical to static data, since there is no experimental way of directly measuring the Parisi function. Its indirect determination through equation (4) would thus be a major result, as pointed out in [3]. It is the principal aim of this paper to discuss the issue of what is precisely determined from a dynamical measurement performed in a physically accessible time window.

Dynamic results have been numerically obtained in many different glassy models, as reviewed in [13]. More recently, experiments have also been able to independently probe two-time susceptibilities and correlations in a number of glassy materials [16–19]. The standard way to present data and test equation (3) is to build an 'FD plot' of the susceptibility $\chi(t_1, t_2)$ as a function of the correlation function $C(t_1, t_2)$, parametrized by the time difference $t_1 - t_2$, conventionally taken as positive [11]. If equation (3) holds, one gets indeed

$$\chi(t_1, t_2) = \frac{1}{T} \int_{C(t_1,t_2)}^1 {\rm d}q\, X(q) \tag{10}$$

implying that the $\chi(C)$ relation is independent of time, and has a slope related to the FDR,

$$\frac{\partial \chi}{\partial C} = -\frac{X(C)}{T}. \tag{11}$$

We have implicitly assumed that $C(t_1, t_1) = 1$ to simplify the notation. It is important to note that neither simulations nor experiments have ever reported an asymptotic FD plot, i.e., a time-independent relation between χ and C. Quite strikingly then, physically accessible time scales are such that equation (3) is not valid. As a consequence, it is necessary to theoretically investigate preasymptotic behaviours where times are large, but finite. Equivalently for the driven dynamics, the case of small but finite driving forces has to be considered.

Far less works have investigated the validity of equation (4). Numerically, it is possible to compute the Parisi function in an equilibrium simulation, obtaining thus the function $P(q, L)$, where L is the—necessarily finite—linear size of the system. The L-dependence is explicitly kept since it is again important to note that no numerical work has yet been able to report the asymptotic form of this function, $P(q, L \to \infty)$, in a glassy system. Moreover, the system size will play an important role below.

Early studies have then empirically compared static and dynamic data through the comparison of the curves $\chi(C, t_2)$ obtained in the dynamics for times t_2 'as large as possible', to the static curve $S(C, L)$ measured statically in a system of size L 'as large as possible' [20, 21]. We have defined

$$S(C, L) = \frac{1}{T} \int_C^1 \mathrm{d}q \int_0^q \mathrm{d}q' P(q', L). \tag{12}$$

With these definitions, equation (4) can be synthetically rewritten as

$$\chi(C) = S(C) \tag{13}$$

where $S(C) = \lim_{L\to\infty} S(C, L)$.

The remarkable coincidence between static and dynamic data initially found in numerical simulations of finite-dimensional spin glasses in dimensions $d = 3$ and $d = 4$ was first taken as the sign that both quantities had converged to their asymptotic limits [20]. Conclusions on the correct description of the low-temperature phase in spin glasses phase were then drawn [20].

These conclusions were however premature, as strikingly demonstrated in recent experiments which have shown that even in the experimental time window the FD plots still have a clear time dependence [18]. This again emphasizes the necessity of a careful theoretical study of preasymptotic behaviours in order to get a correct interpretation of experimental data. This issue is discussed throughout the rest of the paper.

2. Generalized FDT with space

2.1. What about space? A scaling argument

To understand preasymptotic behaviours, a physical picture of the slow dynamical processes involved in the system is needed, since infinite-range glass models provide us with no relevant prediction in that regime. Unfortunately, due to their mean-field nature, they do not provide us with a clear description of the physics either. One thus has to resort to more phenomenological descriptions.

It is now well established, at least in the case of spin glasses, that slow dynamics is accompanied by the existence of a 'coherence length' scale, ℓ: the larger the coherence length the slower the dynamics. Here, an analogy with coarsening phenomena in non-disordered ferromagnetic systems is quite illuminating. When the coarsening dynamics proceeds, larger and larger magnetized domains are present, and the dynamics indeed becomes slower and slower. The extent to which slow dynamics is always accompanied by a large coherence

length in any glassy material is an important open problem in this field. In this paper, we adopt the point of view that this is indeed the case. See [22, 23] for related discussions.

Using this spatial description of slow dynamics, preasymptotic behaviours were conjectured in [4, 5] to obey a generalization of equation (4). The physical picture is the following. At a given wait time, t_2, of the ageing dynamics, the system becomes locally equilibrated up to a coherence length scale, $\ell(t_2)$. It can thus be seen as a heterogeneous mosaic of independent and quasi-equilibrated sub-systems of size $\ell(t_2)$. Now, a dynamic measurement performed on this mosaic in fact probes an ensemble average over equilibrated systems of finite size $\ell(t_2)$. Translating this idea into an equation, one arrives at the conjecture that the following generalization of equation (4) can be valid [4, 5]:

$$X(C, t_2) = \int_0^C \mathrm{d}q' P(q', L) \qquad L = \ell(t_2) \tag{14}$$

which implies that non-equilibrium properties of the system at time t_2, as encoded in the FDR, are related to the equilibrium properties of a system of finite size $L = \ell(t_2)$, as encoded in the Parisi function. Note also that static and dynamic preasymptotic effects are explicitly present in equation (14), since both finite times, t_2, and sizes, L, are taken into account.

The conjecture (14) was first formulated and tested in [4] in the context of the non-equilibrium critical dynamics of the $2d$ XY model, and further studied in [5, 24] in the numerical simulation of the Ising spin glass in dimension $d = 2$. In both cases, the observed behaviours were by construction preasymptotic, since for both models the true asymptotic behaviour was simple equilibrium with $X(C) = 1$ and $P(q) = \delta(q)$. However, on numerically accessible time scales, a non-trivial behaviour reminiscent of the one observed, say, in realistic spin glasses was found, and the conjectured relation (14) was indeed obeyed to a very good precision.

It is straightforward to obtain the relation corresponding to equation (14) in the case of a driven glassy material:

$$X(C, \varepsilon) = \int_0^C \mathrm{d}q' P(q', L) \qquad L = \ell(\varepsilon) \tag{15}$$

where the relevant control parameter in the dynamics is now the amplitude of the driving force, ε. The advantage of this formulation, as exemplified in the numerical simulations below, is that the dynamics is stationary, so that the coherence length itself does not change during the dynamical measurement, as is the case in the ageing regime.

2.2. Single-site quantities

A different generalization of equation (4) was recently discussed in the literature [9, 10]. Inspired by numerical results obtained in a disordered spin system [9], the argument reviewed in section 1.2 was reformulated using single-site quantities defined for a given sample [10]. Therefore, disordered systems only are concerned by this approach.

Consider the alternative single-site definition of a generalized susceptibility [10],

$$\chi_i^r = \frac{r!}{M^{r-1}} \sum_{a_1 < \cdots < a_r}^{M} \left. \frac{\partial s_i^{a_1} \cdots s_i^{a_r}}{\partial h_{a_1 \cdots a_r}} \right|_{h=0} \tag{16}$$

where M thermodynamically coupled copies of the same system have been introduced, so that s_i^a denotes the value of spin i in the copy a. The role of a small coupling of amplitude k between the M copies is discussed in [10]. Its presence is necessary to properly define single-site overlap distributions $P_i(q)$, although its precise form is inessential.

If an inversion of the limits $M \to \infty, t \to \infty, k \to 0$ and $h \to 0$ is again allowed, then a reasoning analogous to that developed in section 1.2 leads to the equality

$$X_i(C) = \int_0^C \mathrm{d}q' P_i(q') \tag{17}$$

between the single-site FDR and local overlap distributions. The single-site FDR is obtained by averaging local correlation, $C_i(t_1, t_2) = s_i(t_1)s_i(t_2)$, and response functions, $R_i(t_1, t_2) = \partial s_i(t_1)/\partial h_i(t_2)$, over various realizations of the thermal history for a single realization of the disorder. We note finally that the derivation of this local FDT makes use of the same type of (uncontrolled) hypothesis of the global one.

2.3. Single-box quantities

Although equations (17) and (14) are different, they are also consistent, because equation (17) physically follows from the concept of a local equilibration in space, so that dynamical properties at site i can be linked to static properties at the same site i.

The disadvantage of this single-site formulation is however evident, since it entirely relies on the presence of quenched disorder in the system. A slight generalization of equation (17) would be to consider single-box quantities instead of single site to get similarly

$$X_i^v(C) = \int_0^C \mathrm{d}q' P_i^v(q') \tag{18}$$

where the box FDR $X_i^v(C)$ is defined from box dynamical functions, $C_i^v(t_1, t_2) = v^{-1} \sum_j s_j(t_1)s_j(t_2)$ and $\chi_i^v(t_1, t_2) = v^{-1} \sum_j \partial s_j(t_1)/\partial h_j(t_2)$, and the sums run over a box of finite volume v centred around site i [6–8]. The corresponding static box-overlap distribution is defined as [25]

$$P_i^v(q) = \lim_{N\to\infty} \left\langle \delta\left(\frac{1}{v} \sum_{j=1}^{v} s_j^\alpha s_j^\beta - q \right) \right\rangle \tag{19}$$

using the same notation as in (5). The interesting point of the formulation (18) is that it should become independent of the considered site i for a sufficiently large box volume v. A second interesting point is that it suggests an alternative to equations (14) and (15), namely

$$X(C, t_2) = \int_0^C \mathrm{d}q' P^v(q) \qquad v = \ell^d(t_2) \tag{20}$$

for the ageing case, and

$$X(C, \varepsilon) = \int_0^C \mathrm{d}q' P^v(q') \qquad v = \ell^d(\varepsilon) \tag{21}$$

for the driven case.

3. Simulations of ageing and driven dynamics

We now turn to a numerical investigation of the two relations (14) and (15) discussed in the preceding section. We first present the model studied and some technical details, before giving our results both for a driven and an ageing dynamics.

3.1. Model and details of the simulations

In this section, we study numerically the Edwards–Anderson model of a spin glass defined by the Hamiltonian [26]

$$H = -\sum_{\langle i,j \rangle}^{N} J_{ij} s_i s_j \tag{22}$$

where s_i ($i = 1, \ldots, N$) are $N = L^d$ Ising spins located at the sites of a cubic lattice when $d = 3$, or a hypercubic lattice when $d = 4$, of linear size L. The coupling constants J_{ij} are random Gaussian variables of mean 0 and variance 1 and the sum in (22) runs over nearest neighbours. We use a standard Monte Carlo algorithm where the spins are randomly updated. Times are given in Monte Carlo steps, where one step represents N attempts to update a spin. Sizes are given in units of the lattice spacing. To study the dynamics of the system, a large system size, $L = 40$ ($d = 3$) and $L = 24$ ($d = 4$), is chosen, so that few realizations of the disorder are needed, typically 10. Such large sizes are necessary, as figure 1 discussed below will clearly demonstrate. This implies that conclusions drawn for systems as small as $L = 10$ have to be taken with much caution [27].

The ageing dynamics is simulated by preparing the system at initial time in a random configuration, thus mimicking an infinite-temperature state. The temperature is then changed at time $t = 0$ to its final value. We will present below data for the temperature $T = 0.7T_c$ in both $d = 3$ and $d = 4$, where $T_c = 0.95$ and $T_c = 1.8$, respectively. Dynamical measurements are then performed during the resulting ageing process.

To simulate the driven dynamics, we use the same type of perturbation as in [15]. On each link (i, j) of the lattice, a coupling $\tilde{J}_{ij}$ is added, where $\tilde{J}_{ij}$ is drawn from a Gaussian distribution of mean 0 and variance ε, which defines then the amplitude of the driving mechanism. The key information about the $\tilde{J}$ is that they are chosen to be antisymmetric, $\tilde{J}_{ij} = -\tilde{J}_{ji}$, which implies that their effect cannot be incorporated in a Hamiltonian force of the type (22). Hence, the effect of the $\tilde{J}$ is that of a non-conservative force, and the system is thus externally driven. As a result, a driven stationary state is reached at sufficiently large times, even for temperatures below T_c: ageing is stopped by the driving force [15]. In that case, measurements are performed in the stationary regime, meaning that a considerable amount of the data corresponding to transient behaviours have to be discarded.

In both cases, dynamical measurements consist of the measurements of the global functions (1) and (2). Since these measurements are by now classic, we do not discuss them further here [13].

In order to perform a comparison with static data, we shall make use of the published equilibrium data of [28] in $d = 3$ and [29] in $d = 4$. Fortunately, box-overlap data exist in $d = 3$ and we shall also make use of them [25].

3.2. Time is length

To accurately test relations (14) and (15), the following steps must be followed.

- Identify and measure in the dynamics the coherence length ℓ.
- Measure global correlation and response functions, from which the corresponding FD plot is built.
- Measure in equilibrium simulations the overlap distribution functions.
- Compare static and equilibrium data with carefully chosen values of the parameters (size, time, driving force), as suggested by equations (14) and (15).

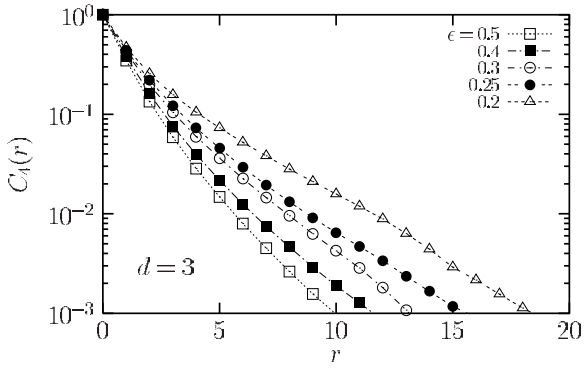

Figure 1. The correlation function (23) for $d = 3$, $T = 0.7T_c$ and various amplitudes ε of the driving force.

The first point, the identification of a coherence length, has been discussed for the ageing dynamics of the Ising spin glass in various dimensions in [30–32], so that the existence, temperature and wait time behaviour of this quantity are well characterized.

To the best of our knowledge, no such results are available for the driven dynamics. We have thus measured in the driven stationary state the standard four-spin correlation function [30]:

$$C_4(r) = \frac{1}{N}\sum_{i=1}^{N} \overline{\langle s_i^a s_{i+r}^a s_i^b s_{i+r}^b \rangle} \tag{23}$$

where the overline means an average over the disorder, and (a, b) are two independent copies of the system. Some corresponding curves are shown in figure 1, for $d = 3$. Very similar results are also obtained for $d = 4$. The features observed in this figure are expected. The amplitude of the driving force is known to control the relaxation time, $t_{\rm rel} = t_{\rm rel}(\varepsilon)$, of the system, the smaller the ε the larger the $t_{\rm rel}$ [15]. From figure 1, we recognize that a slower dynamics also implies the existence of a larger coherence length, $\ell(\varepsilon)$, as revealed by a slower spatial decay of $C_4(r)$.

A non-ambiguous definition of the coherence length is obtained, as in the ageing regime, through the study of the scaling properties of $C_4(r)$. For the ageing, it is known that the correlation (23) is well described by the scaling form [32, 33]

$$C_4(r) \approx \frac{1}{r^{\alpha(T)}}\mathcal{C}\left(\frac{r}{\ell}\right) \tag{24}$$

which can be seen as the definition of the coherence length ℓ. We find that the same scaling behaviour (24) is obeyed in the driven dynamics as well, with the same value of the temperature-dependent exponent $\alpha(T)$ as in the ageing regime. As an example, we report the scaled data for $T = 0.7T_c$ and $d = 3$ in figure 2. We find that the scaling function $\mathcal{C}(x)$ is well described by a simple exponential form, $\mathcal{C}(x) = \exp(-x)$. This contrasts with the 'compressed' exponential form reported in the ageing regime [32]. We have no explanation for this difference, which is however inessential.

The results of figures 1 and 2 allow us to obtain the relationship between the coherence length ℓ and the amplitude of the driving force, ε. From the time dependence of the correlator (1), it is also possible to extract a relaxation time, $t_{\rm rel}(\varepsilon)$. It is thus natural to eliminate ε to obtain the relationship between time and length. Not surprisingly, we find that the relation

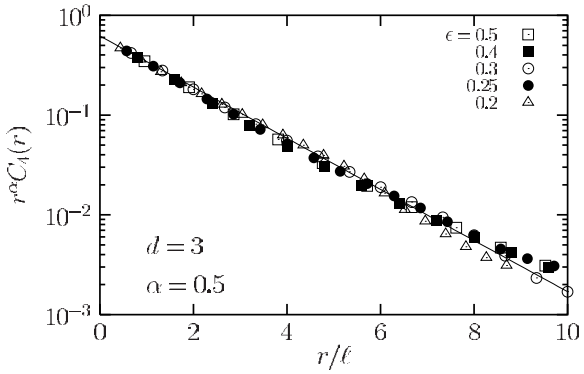

Figure 2. The data of figure 1 rescaled according to equation (24) with $\alpha = 0.5$, $T = 0.7T_c$, $d = 3$. The straight line indicates a simple exponential behaviour of the scaling function $\mathcal{C}(x) = \exp(-x)$.

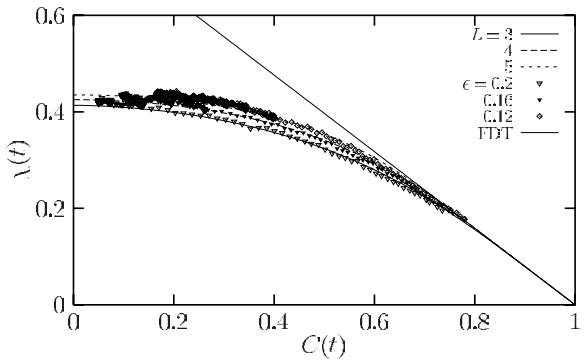

Figure 3. Test of the static–dynamic relationship (15) for the driven dynamics for $d = 4$ and $T = 0.7T_c$. The points are dynamic FD plots, the lines are the double integral of the Parisi function measured in equilibrium simulations.

$\ell(t_{\rm rel})$ in the driven regime, is well compatible with the relation $\ell(t_2)$ measured in the ageing regime at the same temperature.

Although this coincidence might seem anecdotic in this context, we emphasize its physical importance. This suggests indeed that regardless of the control parameter for the dynamics, waiting time or driving force, the dynamics is such that the same dynamic scaling $\ell(t)$ is obeyed: 'Time is length'.

3.3. Generalized FDT for the driven dynamics

Following the programme presented in section 3.2, we compute in the driven dynamics correlations and susceptibilities, and build the corresponding FD plots. Collecting the static data of [25, 28, 29], we are in a position to start and investigate the validity of relations (14), (15), (20) and (21).

We present in figure 3 the results obtained in $d = 4$. In this figure, there are three different FD plots, represented with points, and corresponding to three different values of the driving force, and thus to three different coherence lengths $\ell(\varepsilon)$. The lines correspond to the double integral $S(C, L)$ defined in equation (12) of the Parisi function $P(q, L)$ for three different

system sizes. The agreement between the two sets of curves is extremely good. That this is not a mere coincidence is supported by three important facts.

- The two types of measurements are performed entirely independently, in completely different physical situations.
- The agreement between the two sets of curves is very good on the whole range of the curve, not on a single point. If one recalls that each curve is built from a rather complex manipulation of various quantities without any fitting procedure or free parameter, the agreement becomes much more impressive.
- The coherence lengths measured in the dynamics are $\ell(0.2) = 1.55, \ell(0.16) = 2.0, \ell(0.12) = 2.5$. They are thus in ratio 1:1.29:1.61. The corresponding static length scales are in ratio 1:1.33:1.66. The agreement with the prediction (15) that both lengths should scale similarly is thus clearly excellent.

3.4. Another observable: the link overlap

To test further the hypothesis of a strong link between off-equilibrium properties and static ones resulting from the local equilibration of the material, we focus in this section on a second pair of dynamical observables. Physically, this is motivated by the picture given in section 2.1, where an off-equilibrium system was described as a mosaic of equilibrated sub-systems of size given by the coherence length. A logical consequence is that the link between static and dynamic quantities should exist for all physical observables. This is equivalent to the prediction and test of the unicity of the effective temperature in structural glasses [12, 34–36].

To check this hypothesis, we have investigated the following quantities:

$$C_l(t_1, t_2) = \frac{1}{2Nd} \sum_{i=1}^{N} \sum_{j=1}^{2d}{}' s_i(t_1) s_j(t_1) s_i(t_2) s_j(t_2) \tag{25}$$

$$R_l(t_1, t_2) = \frac{1}{2Nd} \sum_{i=1}^{N} \sum_{j=1}^{2d}{}' \left. \frac{\partial s_i(t_1) s_j(t_1)}{\partial h_{ij}(t_2)} \right|_{h=0} \tag{26}$$

where the prime in the second sum indicates that it is restricted to the nearest neighbours of the site i. The field h_{ij} is thermodynamically conjugated to the observable $s_i s_j$, and can thus be seen as a random perturbation of the coupling constants. From these two dynamical functions, a new FD plot can be built.

Correspondingly, the static quantity to use is the link-overlap distribution function, $P(q_l)$, defined by

$$P(q_l) = \lim_{N\to\infty} \left\langle \delta \left(\frac{1}{2Nd} \sum_{i=1}^{N} \sum_{j=1}^{2d}{}' s_i^\alpha s_j^\alpha s_i^\beta s_j^\beta - q_l \right) \right\rangle. \tag{27}$$

We use here the static data published in [29].

The comparison between the new sets of static and dynamic quantities is reported in figure 4, for the same parameters as in figure 3. It should not come as a surprise that the range of correlators covered by figure 4 is smaller than that covered in figure 3. The long-time limit of the correlator is indeed non-zero in that case.

It is again clear that the agreement between static and dynamic data is very good. The point to emphasize is that for a given amplitude of the driving force, the same size L as in figure 3 is used to compute static data, in agreement with the physical picture described above.

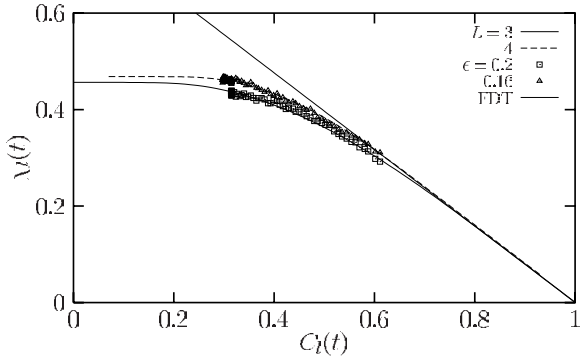

Figure 4. Test of the static–dynamic relationship (15) for the driven dynamics for $d = 4$ and $T = 0.7T_c$ for the link observables. The points are dynamic FD plots, the lines are the double integral of the link-overlap distribution function measured in equilibrium simulations. Note the coincidence between the values of ε and L with those reported in figure 3.

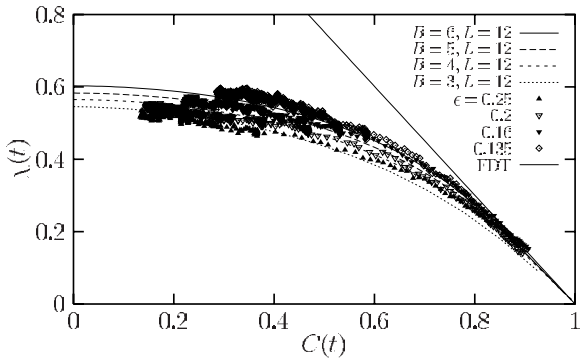

Figure 5. Test of the static–dynamic relationship (21) for the driven dynamics for $d = 3$ and $T = 0.7T_c$. The points are dynamic FD plots, the lines are the double integral of the box-overlap distribution function measured in equilibrium simulations, B refers to the linear size of the box, L to the linear size of the total system.

These results are a striking confirmation of the local equilibration hypothesis formulated in this paper.

3.5. Using the box-overlap distributions

Having established numerically the validity of the relationship between static and dynamic properties in $d = 4$, we now turn to $d = 3$. This will allow us to make use of the box-overlap distribution functions published in [25]. To compute this function, the linear size of the total system was fixed to $L = 12$, and the linear size of the boxes, B, was varied [25].

Our numerical results are reproduced in figure 5, where the FD plots built from the spin–spin dynamical functions (1) and (2) for various amplitudes of the driving force are compared to the static data obtained from the box-overlap distributions.

As for $d = 4$, we find a very good agreement between static and dynamic data. The coherence length scales are in ratio 1:1.35:1.59:1.88, while the sizes of the boxes are in ratio 1:1.33:1.66:2, the coincidence being again satisfying.

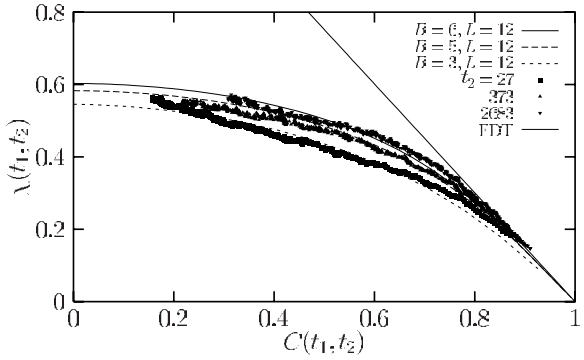

Figure 6. Test of the static–dynamic relationship (20) for the ageing dynamics, for $d = 3$ and $T = 0.7T_c$. The points are dynamic FD plots, the lines are the double integral of the box-overlap distributions measured at equilibrium. The discrepancies for the short waiting time $t_2 = 27$ are discussed in the text.

We conclude that numerical simulations in $d = 3$ and $d = 4$ of the driven dynamics of the Ising spin glass nicely support the theoretical propositions (15) and (21).

3.6. Generalized FDT in ageing dynamics

We conclude the report of our numerical results with a brief mention of the results we have obtained in the ageing regime for $d = 3, 4$. Similar results have already been published, as mentioned above, but the crucial coincidence between time (in the dynamics) and size (in the statics) was not noted, although it was supported by the data [20, 33]. We have also discussed above the results obtained for $d = 2$, when no spin glass phase exists [5, 24].

We give an example of our own data in the ageing regime in $d = 3$ in figure 6. There are four important points we want to make on these data.

First, we make use of the box-overlap distribution function in this figure, which was not the case in previous works. The total overlap distribution functions give however results which are similarly good.

Secondly, the dynamic data can be described using the same equilibrium quantity $P(q, L)$ as for the driven dynamics. This is a clear support of the analytical result that driven and ageing dynamics should give rise to similar deviations from the FDT [12, 14, 15].

Thirdly, we have intentionally included data for a very short wait time, $t_2 = 27$, for which the agreement with equation (20) is not quite as good, to underline the fact that during the dynamical measurements the coherence length itself evolves with time. This was obviously not the case when the driven dynamics was considered. For this short wait time, for instance, the final time is $t_1 = 10^5$, so that we do not expect the FD plot to follow the line built from static data obtained at a given box size corresponding to the earlier time $L = \ell(t_2)$. Indeed, a clear deviation at large times (corresponding to low values of the correlator) is observed. This was anticipated and noted in [4, 5], and was another motivation to focus also on the driven dynamics in this paper.

Fourthly, we have discussed above the link between the coherence length ℓ and the system size or box size in terms of relative ratio. It is clear that an absolute comparison is not possible, since the coherence length has no 'absolute value', in contrast to the box size univocally defined in the static computation. However, the 'large' numerical factor between L and ℓ reported in [20] (about 4 in $d = 3$) was an argument used against the theoretical

proposition (14) formulated in this and previous works [37].[1] It can be seen from figure 6 that the factor between ℓ and B is less than 2 when the box-overlap distribution is used, thus clearly weakening this criticism.

4. Conclusion

In this paper, we have given a scaling argument to support the proposition of [4, 5] to generalize the relationship between the off-equilibrium FDR and the equilibrium overlap distribution to the physically relevant domain of finite times and sizes. Inspired by previous approaches to the asymptotic relation [3, 10], we proposed relations (14) and (15) between the FDR computed at any moment of the dynamics, and the equilibrium box-overlap distribution function, where the size of the box to be used is imposed by the dynamical coherence length.

We have argued that these relations reflect the simpler notions of the local equilibration in space and the dynamical heterogeneity of the system, two ingredients which are inherent to systems with slow dynamics, independently of their space dimensionality, their dynamics or the presence of disorder.

We have emphasized throughout the paper that relations (14)–(15) were the physically relevant ones, as compared to the asymptotic form of equation (4). Hence, they have to be taken into account before drawing conclusions on the equilibrium glass phase one seeks to study [20]. This remark, already made in [4, 5], is repeated here because there recently appeared FD plots built from experimental dynamic measurements in spin glasses [18]. As anticipated [5], these dynamical measurements are very similar to those observed in simulations, despite the enormous difference in time scales between experiments and simulations. This is because the growth of the coherence length is so slow in spin glasses that this difference in time scales reduces to a very modest factor in terms of the coherence length [23, 32, 38]. This in fact implies that the 'finite-size effects' reported in simulations, are present in experiments as well. This points towards the experimental irrelevance of the thermodynamic limit in spin glasses.

Finally, we made clear that relations (14)–(15) do not have the character of a theorem, meaning that more work is needed to assess their range of validity. In particular, coarsening systems are a simple counterexample of this relation. This is due to the fact that the dynamical behaviour is entirely dominated by topological defects which are absent in the equilibrium simulations, so that finite-time dynamics and statics do not coincide [4, 5, 39]. There remains to be seen to what extent this alternative 'defect' description of glassy dynamics generally holds in systems such as supercooled liquids or soft glassy materials. This is certainly a quite challenging issue.

Acknowledgments

M Mézard suggested using the existing numerical results for the box-overlap distributions to weaken the criticism he had himself formulated. I thank E Marinari, J Ruiz-Lorenzo, H Katzgraber, P Young who kindly provided me with their static data [25, 28, 29], and A Barrat, P Holdsworth and M Sellitto for early discussions and collaborations [4, 5]. J Kurchan made important remarks on a previous version of the manuscript and I warmly thank him for this luxury *service après-thèse*. This work is supported by a European Marie Curie Fellowship No HPMF-CT-2002-01927, CNRS (France) and Worcester College Oxford.

[1] M Mézard remarked on this surprisingly large factor, and suggested considering box-overlap distribution functions as a check.

Numerical simulations were started at the PSMN in ENS Lyon (France) and finished on Oswell at the Oxford Supercomputing Center, Oxford University.

References

[1] Young A P (ed) 1997 *Spin Glasses and Random Fields* (Singapore: World Scientific)
[2] Bouchaud J-P, Cugliandolo L F, Kurchan J and Mézard M 1997 *Contribution to Spin Glasses and Random Fields* (Singapore: World Scientific)
[3] Franz S, Mézard M, Parisi G and Peliti L 1998 *Phys. Rev. Lett.* **81** 1758
Franz S, Mézard M, Parisi G and Peliti L 1999 *J. Stat. Phys.* **97** 459
[4] Berthier L, Holdsworth P C W and Sellitto M 2001 *J. Phys. A: Math. Gen.* **34** 1805
[5] Barrat A and Berthier L 2001 *Phys. Rev. Lett.* **87** 087204
[6] Chamon C, Kennett M P, Castillo H and Cugliandolo L F 2002 *Phys. Rev. Lett.* **89** 217201
[7] Castillo H E, Chamon C, Cugliandolo L F and Kennett M P 2002 *Phys. Rev. Lett.* **88** 237201
[8] Castillo H E, Chamon C, Cugliandolo L F, Iguain J L and Kennett M P 2002 *Preprint* cond-mat/0211558
[9] Montanari A and Ricci-Tersenghi F 2003 *Phys. Rev. Lett.* **90** 017203
[10] Parisi G 2002 *Preprint* cond-mat/0208070
Parisi G 2002 *Preprint* cond-mat/0211608
[11] Cugliandolo L F and Kurchan J 1993 *Phys. Rev. Lett.* **71** 173
Cugliandolo L F and Kurchan J 1994 *J. Phys. A: Math. Gen.* **27** 5749
[12] Cugliandolo L F, Kurchan J and Peliti L 1997 *Phys. Rev.* E **55** 3898
[13] Crisanti A and Ritort F 2003 *J. Phys. A: Math. Gen.* **36** R181 (*Preprint* cond-mat/0212490)
[14] Cugliandolo L F, Kurchan J, Le Doussal P and Peliti L 1997 *Phys. Rev. Lett.* **78** 350
Berthier L, Barrat J-L and Kurchan J 2000 *Phys. Rev.* E **61** 5464
[15] Berthier L, Barrat J-L and Kurchan J 2001 *Phys. Rev.* E **63** 016105
[16] Grigera T S and Israeloff N E 1999 *Phys. Rev. Lett.* **83** 5038
[17] Bellon L, Ciliberto S and Laroche C 2001 *Europhys. Lett.* **53** 511
[18] Hérisson D and Ocio M 2002 *Phys. Rev. Lett.* **88** 257202
[19] Buisson L, Garcimartin A and Ciliberto S submitted
Buisson L, Bellon L and Ciliberto S 2003 *J. Phys.: Condens. Matter* **15** S1163
[20] Marinari E, Parisi G, Ricci-Tersenghi F and Ruiz-Lorenzo J J 1998 *J. Phys. A: Math. Gen.* **31** 2611
[21] Ricci-Tersenghi F, Parisi G, Stariolo D A and Arenzon J J 2001 *Phys. Rev. Lett.* **86** 4717
de Candia A and Coniglio A 2001 *Phys. Rev. Lett.* **86** 4716
[22] Tarjus G and Kivelson D 2001 *Jamming and Rheology* ed A Liu and S Nagel (New York: Taylor and Francis)
[23] Berthier L, Viasnoff V, White O, Orlyanchik V and Krzakala F 2002 *Preprint* cond-mat/0211106 (2003 *Slow Relaxation and Nonequilibrium Dynamics in Condensed Matter* ed J-L Barrat, J Dalibard, M V Feigel'man and J Kurchan (Berlin: Springer) at press)
[24] Franz S and Mulet R 2003 *Preprint* cond-mat/0301226
[25] Marinari E, Parisi G, Ricci-Tersenghi F and Ruiz-Lorenzo J J 1998 *J. Phys. A: Meth. Gen.* **31** L481
[26] Edwards S F and Anderson P W 1975 *J. Phys. F: Met. Phys.* **5** 965
[27] Stariolo D A 2001 *Europhys. Lett.* **55** 726
[28] Marinari E, Parisi G and Ruiz-Lorenzo J J 1998 *Phys. Rev.* B **58** 14852
[29] Katzgraber H G, Palassini M and Young A P 2001 *Phys. Rev.* B **63** 184422
[30] Kisker J, Santen L, Schreckenberg M and Rieger H 1996 *Phys. Rev.* B **53** 6418
[31] Komori T, Yoshino H and Takayama H 1999 *J. Phys. Soc. Japan* **68** 3387
[32] Berthier L and Bouchaud J-P 2002 *Phys. Rev.* B **66** 054404
[33] Marinari E, Parisi G, Ricci-Tersenghi F and Ruiz-Lorenzo J J 2000 *J. Phys. A: Math. Gen.* **33** 2373
[34] Fielding S M and Sollich P 2002 *Phys. Rev. Lett.* **88** 050603
[35] Berthier L and Barrat J-L 2002 *Phys. Rev. Lett.* **89** 095702
Berthier L and Barrat J-L 2002 *J. Chem. Phys.* **116** 6228
[36] Mayer P, Berthier L, Garrahan J P and Sollich P 2003 *Phys. Rev.* E at press (*Preprint* cond-mat/0301493)
[37] Mézard M 2001 Private communication
[38] Berthier L and Holdsworth P C W 2002 *Europhys. Lett.* **58** 35
[39] Godrèche C and Luck J-M 2000 *J. Phys. A: Math. Gen.* **33** 1151
Lippiello E and Zannetti M 2000 *Phys. Rev.* E **61** 3369